Electrochemical Methods for Quantitative Estimation of Ambroxol Hydrochloride in drug for the Treatment of Asthmatic Bronchitis

Lina Li

Medical School, Xuchang University, Xuchang, 461000 China
E-mail: LinaLi02@hotmail.com, lilina7188@163.com

This study presented the electrochemical quantitative estimation of ambroxol hydrochloride (AHC) as drug safety for asthmatic bronchitis on ZnO nanoparticles electrodeposited on carboxylated CNTs modified glassy carbon electrode (ZnO NPs/c-CNTs/GCE). The electrodeposition technique was applied for the preparation of the ZnO NPs/c-CNTs/GCE. The structural and morphological analyses using FESEM and XRD showed ZnO NPs in hexagonal wurtzite crystal structure electrodeposited on the twisted and wrapped tubular structure of c-CNTs. The electrochemical study using the CV technique showed that ZnO NPs/c-CNTs/GCE indicated lower peak potential, higher sensitivity and stability than c-CNTs/GCE and ZnO NPs/GCE due to the synergetic effect of ZnO NPs and c-CNTs. The studies of interference and concentration effects using DPV technique showed to the selective response of ZnO NPs/c-CNTs/GCE to the electrochemical determination of AHC, and the linear range, sensitivity and detection limit were obtained 1 to 120 μM, 10.7393μA/μM and 0.02 μM, respectively. The practical ability of ZnO NPs/SWCNTs modified GCE was investigated for the determination of AHC content in ambroxol hydrochloride syrup as a real sample. The results evidenced to good precision and appropriate validity for practical analyses in pharmaceutical samples.

1. INTRODUCTION

Acute bronchitis as a respiratory disease is a type of chest cold that the inflammation in the bronchi cause to respiratory congestion, difficulty breathing, wheezing, coughing up mucus, chest pain and fever, tightness [1-3]. In addition, asthma is an inflammatory condition that leads to tightening of the muscles around the airways and swelling that cause airways to narrow, thereby patient attempts to draw in more oxygen through tightened passageways [4, 5]. Asthmatic bronchitis is bronchitis that occurs as a result of asthma or incidence of both acute bronchitis and asthma together [6-8].

Int. J. Electrochem. Sci., 16 **(2021)** Article ID: 210917

2

Ambroxol hydrochloride (AHC, 4-[(2-amino-3,5-dibromophenyl) methylamino] cyclohexan-1-ol;hydrochloride) as an aromatic amine is a phlegm dissolving agent. Studies have been shown that AHC as a conventional treatment can improve the therapeutic of asthmatic bronchitis [9, 10]. AHC as a new type of expectorant medication can stimulate the production of mucus and respiratory tract through regulating mucus viscosity, serous secretion and mucinous secretion [11-13]. Therefore, many researchers have been focused on synthesis and determination AHC in pharmaceutical dosage and biological sample through the spectrophotometry, high-performance liquid chromatography, gas chromatography, colorimetry and electrochemical methods [14-16]. Among them, electrochemical methods such as potentiometry, amperometry and voltammetry have been shown to high sensitivity and low detection limit [17-19]. However, the modification of electrode surface with nanomaterial and composites in electrochemical cells can improve the linear range and stability of sensors [20-22]. Adequate studies have not yet been performed to promote the stability and linear range of AHC sensors. Therefore, this study was carried out to quantitative estimation of AHC in drug safety for asthmatic bronchitis on ZnO NPs/c-CNTs/GCE.

2. MATERIALS and METHOD

Prior to the modification of GCE, the electrode surface was first hand-polished with 0.3 and 0.05 alumina slurry (99.99 %, Sigma-Aldrich) on a polishing cloth for 10 minutes, respectively, until the electrode surface reached a mirror finish. Then, it was thoroughly rinsed with deionized (DI) water, and sonicated in a mixture of DI water and pure ethanol (volume ratio 1:1) for 10 minutes.

The acid treatment via an oxidation process was used for purification and carboxylation of CNTs (99%, Qingdao Haoyu Graphite Products Co., Ltd., China) in 4 M acid solution of H_2SO_4/HNO_3 with a volume ratio of 1:3 [23] for 4 hours. This process caused to form of carboxylic acid COOH groups on the CNTs (c-CNTs). Then, c-CNTs were electrodeposited on GCE through electrochemical reduction process on Autolab with potentiostat/galvanostat (PGSTAT30, Utrecht, The Netherlands) using a conventional three-electrode cell, containing the clean GCE, Ag/AgCl/ saturated electrode, Pt wire as the working, reference and counter electrodes, respectively. The electrodeposition was carried out at a constant potential of -1.85V for 5 minutes in the electrolyte which contained 15mg/L of c-CNTs and 15mg/L $MgSO_4$ (99%, Shandong Hairun New Material Technology Co., Ltd., China) [24]. After that, the c-CNTs/GCE was rinsed with DI water.

The electrodeposition of ZnO NPs on GCE and c-CNTs/GCE was performed in a aqueous solution containing 0.5 M $ZnCl_2$ (98%, Merck) and 0.1 M KNO_3 (99.99%, Sigma-Aldrich) in equal volume at 50 °C using Autolab system at -0.7V for total duration of 8 minutes [24]. Next, for oxidation and stabilization of the electrochemical properties, the obtained Zn NPs/GCE and Zn NPs/c-CNTs/GCE, the modified electrodes were immersed in 0.07 M NaOH (99%, Xinjiang Zhongtai Import And Export Co., Ltd., China) solution under applying the cycling potential between 0.05 and 0.75 V for 5 minutes at a scan rate of 20mV/s. Finally, the modified ZnO NPs/GCE and ZnO NPs/c-CNTs/GCE was washed with DI water.

For the preparation of the pharmaceutical sample, ambroxol hydrochloride syrup was purchased from a local pharmacy that every 5 ml of syrup contains 15 mg of AHC (3mg/ml). For determination of the AHC content in the purchased syrup, an accurately weighted portion of syrup was mixed with 0.1 M phosphate buffer solutions (PBS) pH 7 in an equal volume ratio, and then the DPV measurement was applied to detect the initial AHC in the prepared real pharmaceutical specimen. The standard addition of AHC was used to determine recovery and relative standard deviation (RSD).

Cyclic voltammetry (CV) and differential pulse voltammetry (DPV) for electrochemical studies of prepared electrodes were carried out using a potentiostat (Autolab, Metrohm, PGSTAT302N, EcoChimie B.V., Utrecht, The Netherlands) in standard a three-electrode system containing the working electrode (prepared electrodes), counter electrode (platinum wire) and reference electrode (Ag/AgCl). 0.1 M PBS was used as an electrolyte for electrochemical studies which prepared from 0.1 M H_3PO_4 (99%, Sigma-Aldrich) and 0.1 M NaH_2PO_4 (99%, Sigma-Aldrich).

Field emission scanning electron microscopy (FESEM SU-8000, Hitachi, Tokyo, Japan) and X-ray diffraction (XRD, Bruker-AXS, Billerica, MA, USA) techniques were applied to characterization the structural and surface morphologies of the prepared electrodes.

3. RESULTS and DISCUSSION

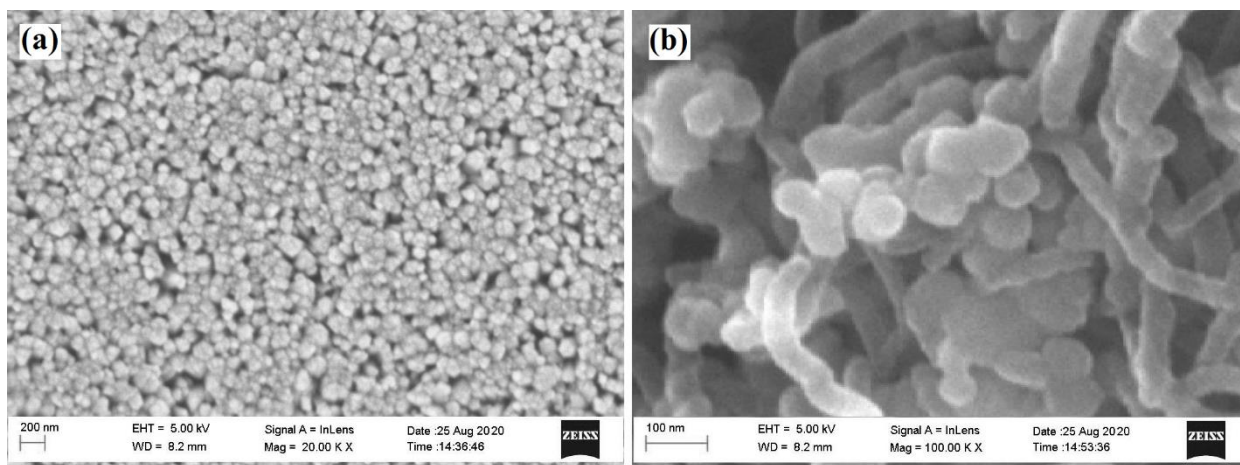*3.1 Structural characterization of modified electrodes*

Figure 1. SEM image of (a) ZnO NPs/GCE, (b) c-CNTs/GCE (c) ZnO NPs/c-CNTs/GCE

The morphology of ZnO NPs/GCE and ZnO NPs/c-CNTs/GCE are shown in FESEM images of Figure 1. As seen from Figure 1a, For Electrodeposited the ZnO NPs on GCE, the ZnO NPs with the average size of 90nm were formed on electrode surface. FESEM image of ZnO NPs/c-CNTs/GCE in Figure 1b shows ZnO NPs covered the c-CNTs and dispersion of nanoparticles is controlled by surface functionalization [25]. The carboxyl groups on c-CNTs walls interact inter/intermolecular through hydrogen bonding with the oxygen of the ZnO or the oxygen atoms of carboxyl groups interact with Zn atoms leads to the formation of the high stale nanostructured film on GCE [26, 27].
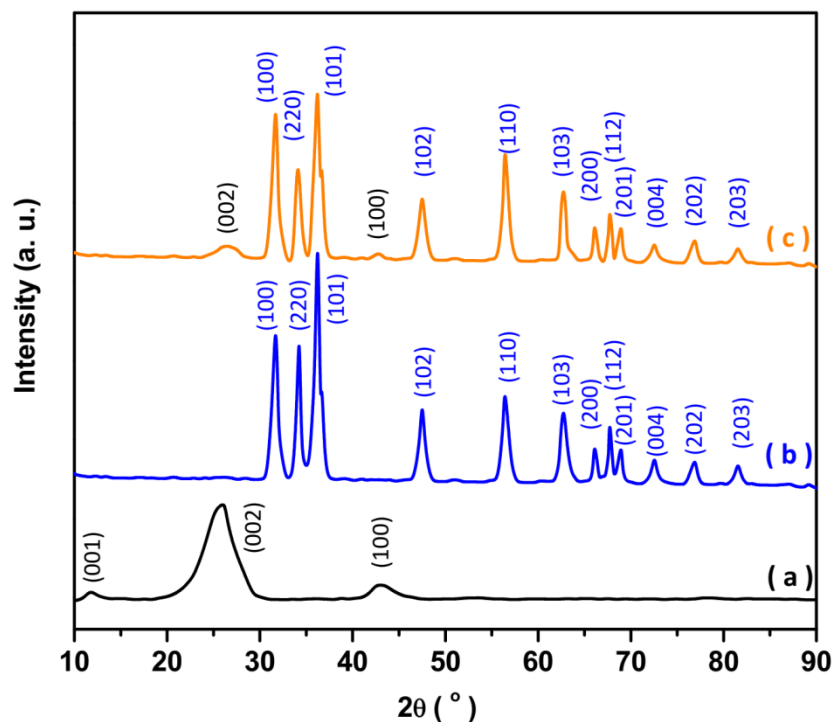
Figure 2. XRD patterns of (a) ZnO NPs, (b) c-CNTs, and (c) ZnO NPs/c-CNTs.

The structural characterization of powders of electrodeposited films using XRD is shown in Figure 2. As observed from XRD pattern of c-CNTs Figure 2a, the diffraction peaks are at 11.90°, 25.69°, and 43.10 that these corresponded to the (001), (002), and (100) planes of graphitic carbon (JCPDS Card number 28-1192), respectively. The XRD pattern of ZnO and ZnO NPs/c-CNTs in Figures 2b and 2c reveals the diffraction peaks at 31.65°, 34.31°, 36.20°, 47.59°, 56.44°, 62.89°, 66.13°, 67.60°, 68.83°, 72.49°, 76.83°, and 81.59° that all of these peaks are assigned to the hexagonal wurtzite crystal structure of ZnO with (100), (002), (101), (102), (110), (103), (200), (112), (201), (004), (202) and (203) planes (JCPDS No. 36-1451), respectively [28, 29]. In addition, the XRD pattern of ZnO NPs/c-CNTs shows additional peaks at 25.97° and 43.02 which related to strong anchoring of electrodeposited ZnO NPs on c-CNTs. Moreover, these results suggest that the hexagonal wurtzite crystal structure of ZnO remains unchanged during the electrodeposition process on the c-CNTs.

3.2 Electrochemical study of prepared electrode for determination of AHC

For electrochemical characterization of the response of GCE, c-CNTs/GCE, ZnO NPs/GCE and ZnO NPs/c-CNTs/GCE, the CV curves of electrodes are shown in Figure 3a in 0.1M PBS at a 10 mV/s scan rate in 0-1.5V potential range in absence and presence of 0.15 μM AHC. It is found that all electrodes do not show any redox peaks in absence of AHC. After the addition of 1μM AHC solution in an electrochemical cell, CV curves in Figure 3b display single anodic peak at 0.95 V, 0.80 V, 0.78 V and 0.72 V for GCE, c-CNTs/GCE, ZnO NPs/GCE and ZnO NPs/c-CNTs/GCE, respectively. The

GCE shows the weak and broader peak that it reflects to its sluggishness in electron transfer kinetics and hindrance the sensitivity. It is observed that the anodic peak on the CV of c-CNTs/GCE are about two times and three times more than that of ZnO NPs/GCE and GCE, respectively, which can highlight the CNTs effect on the improvement of electrochemical behavior because of its significant electrochemical conductivity, small bandgap (1.1eV) [30], and high surface area and activated nano-size sites for AHC loading [31-34]. These properties of CNTs can facilitate the electron transfer between the AHC and the electrode surface. Furthermore, the CV curve of ZnO NPs/c-CNTs/GCE shows the highest current at the lowest potential. This enhancement can be related to strong interaction between the ZnO NPs and c-CNTs through electrochemical bonds and p–π stacking/electrostatic interaction and ZnO NPs are directly coupled with C in the continuous chain of c-CNTs lattice [35, 36]. According to the FESEM analyses, the ZnO NPs and c-CNTs modified GCE provide a highly porous and high effective surface area. Therefore, the synergetic effect of ZnO NPs and c-CNTs promote sensitivity and the electron transfer kinetics in the electrochemical response of ZnO NPs/c-CNTs/GCE to determine AHC.
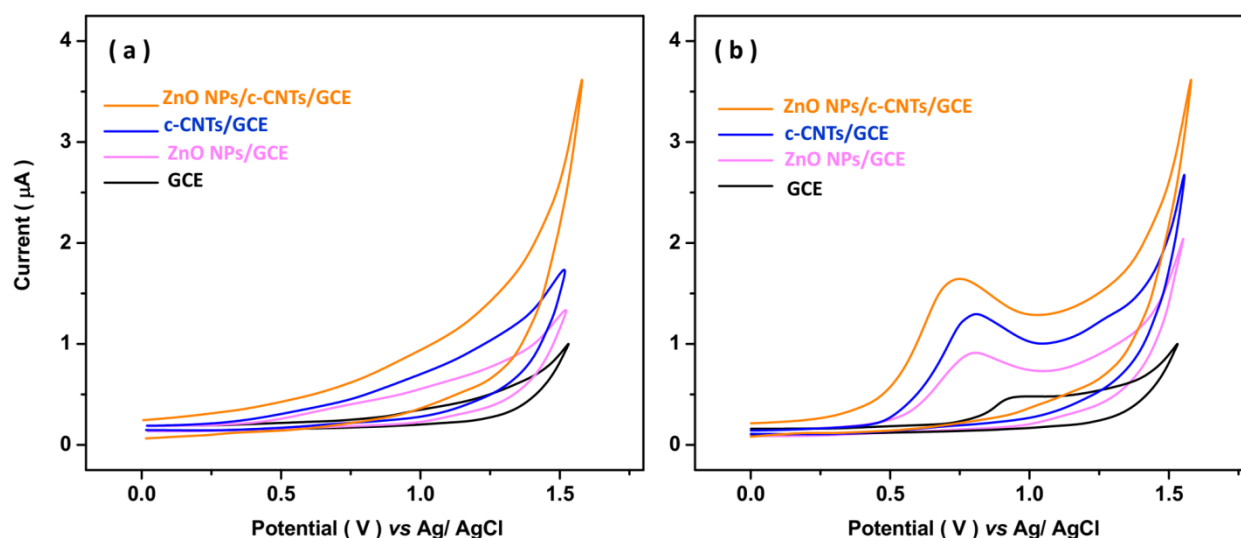

Figure 3. The CV curves of GCE, c-CNTs/GCE, ZnO NPs/GCE and ZnO NPs/c-CNTs/GCE in 0.1M PBS at a 10 mV/s scan rate in 0-1.5V potential range in (a) absence and (b) presence of 0.15 µM AHC.

Furthermore, the electrochemical investigation was carried out to examine the stability of response of modified electrodes to the addition of AHC using record continues CV of electrodes in 0.1 M PBS pH 7.0 at a scan rate of 10 mV/sin presence of 0.15 µM AHC. Figure 4 shows the initial and 80th recorded CV of all electrodes in presence of 0.15 µM AHC solution, indicating to decrease of peak currents 30%, 19%, 8%, and 4% after 80th CVs for GCE, c-CNTs/GCE, ZnO NPs/GCE and ZnO NPs/c-CNTs/GCE, respectively. Therefore, ZnO NPs/c-CNTs/GCE displays the high sensitivity and chemical stability due to corrosion resistance of CNTs and ZnO [37, 38], and as consequently it was used as an appropriate electrode for following electrochemical study AHC.
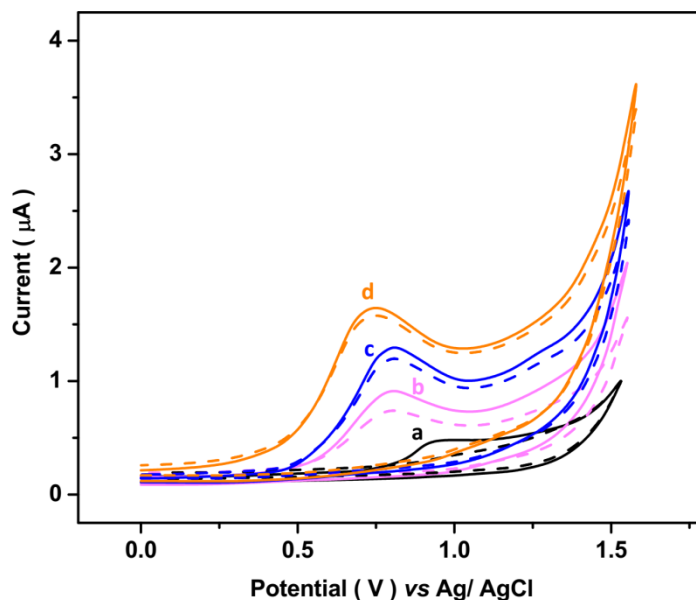
Figure 4. The initial (solid line) and 80th (dash line) CV curves of (a) GCE, (b) c-CNTs/GCE, (c) ZnO
NPs/GCE and (d) ZnO NPs/c-CNTs/GCE in 0.1M PBS at a 10mV/s scan rate in 0-1.5V
potential range in presence of 0.15 μM AHC.

In order to study the AHC concentration effect on electrochemical DPV results of ZnO NPs/c-CNTs/GCE to successive additions of 10 μM AHC solutions in 0.1M PBS at a 10 mV/s scan rate in 0-1.5V potential range. As seen from Figure 5a, the DPV curves exhibit an oxidation peak at 0.72 V and electrocatalytic current is enhanced by increasing the AHC concentration in the electrochemical cell which evidence of the electrochemical activity of the proposed electrode as an AHC sensor. The resulted calibration plot in Figure 5b shows the linear relationship between the electrocatalytic response and AHC concentration from 1 to 120 μM. Moreover, the detection limit and sensitivity are evaluated 0.02 μM and 10.7393μA/μM, respectively. Table 1 displays the obtained value of the linear range, sensitivity and detection limit of this study and different AHC electrochemical sensors. As seen, the ZnO NPs/c-CNTs/GCE as low cost, eco-friendly and simple and easy-to-make AHC sensors showed comparable performance to other electrodes. The obtained detection limit and linear range are lower and broader than other reported values in Table 1, respectively. The high electrostatic affinity between ZnO NPs and c-CNTs network lead to improve direct electron transfer where ZnO NPs/c-CNTs electrode modified with the satisfactory group on conductive nano-materials to enhance the surface infrastructure to transfer electrons directly from the analyte in the electrolyte to the electrode surface [37]. Comparison between the sensitivity of sensors reveals that the only Ruthenium doped TiO$_2$ NPs /rGO/CPE [19] as more expensive sensor shows the higher sensitivity than ZnO NPs/c-CNTs/GCE and other presented sensors [17, 18, 39, 40] have lower sensitivity. The significant role of c-CNTs in the improvement of sensing properties of ZnO NPs/c-CNTs/GCE can be obviously found by considering the sensing properties of ZnO NPs/CPE [17]. Therefore, the results of comparison confirm that ZnO NPs/c-CNTs/GCE can be considered as low-cost and eco-friendly AHC sensors.
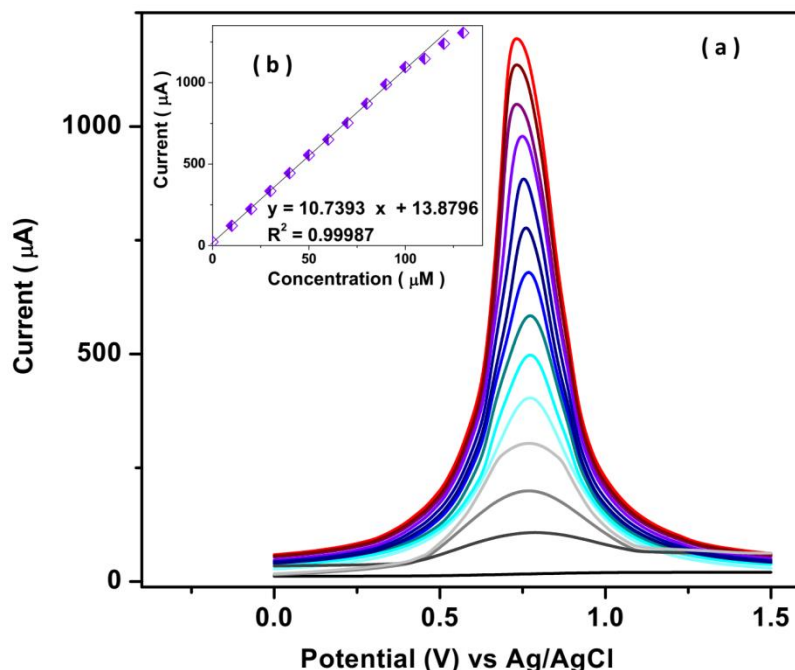
Figure 5. (a) The electrochemical DPV results of ZnO NPs/c-CNTs/GCE to successive additions of 10 μM AHC solutions in 0.1M PBS at a 10mV/s scan rate in 0-1.5V potential range.; (b) the calibration plot.

Table 1. The obtained value of linear range, sensitivity and detection limit of this study and different AHC electrochemical sensors

Electrodes	Technique	Linear range (μM)	Sensitivity (μA/μM)	detection limit (nM)	Ref.
ZnO NPs/ CPE	DPV	0–0.8	10.57	1.4	[17]
TiO$_2$ NPs/ CPE	DPV	1–30	2.2	9.9	[18]
Ruthenium doped TiO$_2$ NPs /rGO/CPE	SWV[a]	0.1 –0.6	271.47	1.0	[19]
boron-doped diamond electrode	SV[b]	0.05–0.7	2.045	10	[39]
GCE	DPV	10–100	0.067	940	[40]
CPE	SSV[c]	0.03–0.4	-	5.4	[41]
MWCNT/Nafion/GCE	DPV	0.01-1.8	-	1	[42]
ZnO NPs/c-CNTs/GCE	DPV	1-120	10.7393	0.02	This work

For study the selectivity of ZnO NPs/c-CNTs/GCE to determination AHC, the components syrup of ambroxol hydrochloride, containing terbutaline (TE), guaiphenesinsulphate (GS) and menthol (ME) were selected as interferent agents in electrochemical analysis of AHC. Moreover, the interfering

effect of 10 µM Fe^{3+}, Cu^{2+}, Mn^{2+}, Cl^-, CO_3^{2-}, ClO_3^-, NO_3^-, S^{2-}, PO_4^{3-}, SO_4^{2-} and CH_3COO^- was also investigated through the DPV analysis in 0.1 M PBS pH 7.0 at a scan rate of 10 mV/s in the potential range of 0 to 1.5 V. Figure 6 depicts the recorded electrocatalytic current at 0.72 V which indicated an obvious signal to additions of 1 µM AHC solution (10.89 µA) and there aren't any significant electrocatalytic response in successive addition of 10 µM of selected interferent agents in the electrochemical cells. These observations are confirmed the selective behavior of ZnO NPs/c-CNTs/GCE to the electrochemical determination of AHC. Moreover, the last injection of 1 µM AHC solution shows the electrocatalytic current of 10.74 µA which indicated to good repeatability of proposed sensor.
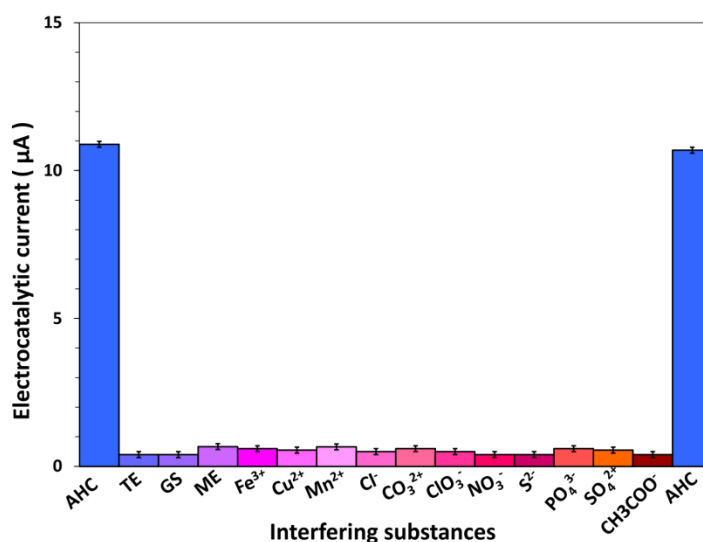

Figure 6. The recorded electrocatalytic current of ZnO NPs/SWCNTs/GCE through the DPV analysis in 0.1M PBS at a 10mV/s scan rate at 0.72 V in successive additions 1 µM of AHC and 10 µM of interferent solutions.

The practical ability of ZnO NPs/SWCNTs/GCE was studied for the determination of AHC content in ambroxol hydrochloride syrup. Figure 7 shows the obtained DPV curves and calibration plot in the prepared real sample that prepared in 0.1 M PBS pH 7 in equal volume ratio at a 10mV/s scan rate in 0-1.5V potential range in successive additions 1mg/ml AHC solutions. The calibration plot shows that the AHC content in syrup is obtained 2.94 mg/ml which is in agreement with the labeled value of syrup. Table 2 shows the recovery and RSD values which can be attributed to good precision and appropriate validity for practical analyses in pharmaceutical samples.
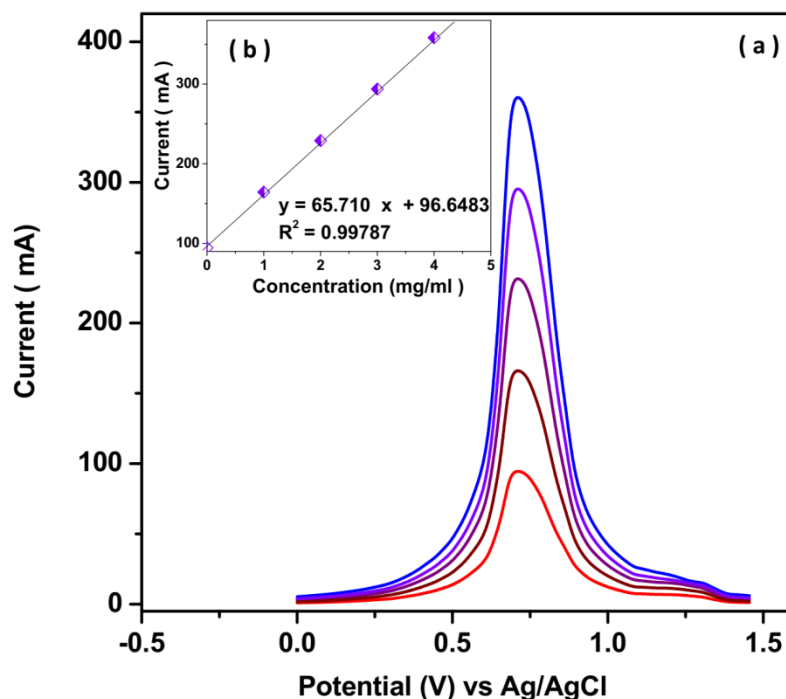
Figures 7. (a) The DPV curves of ZnO NPs/SWCNTs/GCE in real sample in 0.1M PBS at a 10mV/s scan rate in 0-1.5V potential range in successive additions 1mg/ml AHC solutions; (b) calibration plot.

Table 3. Analytical results of ZnO NPs/SWCNTs/GCE to detection AHC in prepared real samples of AHC syrup.

Added (mg/ml)	Found (mg/ml)	Recovery (%)	RSD (%)
1.00	0.99	99.0	4.11
2.00	1.98	99.0	3.21
3.00	2.87	95.6	3.55
4.00	3.97	99.2	4.25

4. CONCLUSION

This study was carried out for electrochemical quantitative estimation of AHC on ZnO NPs/c-CNTs/GCE. The electrodeposition method was applied for preparation of the ZnO NPs/c-CNTs/GCE. FESEM and XRD analyses showed ZnO NPs in hexagonal wurtzite crystal structure covered the twisted and wrapped tubular structure of c-CNTs. The electrochemical study of c-CNTs/GCE, ZnO NPs/GCE and ZnO NPs/c-CNTs/GCE for determination of AHC showed that ZnO NPs/c-CNTs/GCE indicated lower peak potential, higher sensitivity and stability than c-CNTs/GCE and ZnO NPs/GCE due to the synergetic effect of ZnO NPs and c-CNTs. The studies of interference and concentration effects revealed to selective behavior of ZnO NPs/c-CNTs/GCE to the electrochemical determination

Int. J. Electrochem. Sci., 16 **(2021)** Article ID: 210917

10

of AHC and the linear range, sensitivity and detection limit were evaluated 0.02 µM, 10.7393µA/µM and1 to 120 µM, respectively. The practical ability of ZnO NPs/SWCNTs/GCE was studied for determination of AHC content in ambroxol hydrochloride syrup as real sample and results indicated to good precision and appropriate validity for practical analyses in pharmaceutical samples.

References

1. Q. Zou, P. Xing, L. Wei and B. Liu, *Rna*, 25 (2019) 205.
2. Q. Jiang, G. Wang, S. Jin, Y. Li and Y. Wang, *International journal of data mining and bioinformatics*, 8 (2013) 282.
3. X. Pang, K. Gong, X. Zhang, S. Wu, Y. Cui and B.-Z. Qian, *Pharmacological research*, 144 (2019) 235.
4. J. Hu, M. Wang, C. Zhao, Q. Pan and C. Du, *Science China Technological Sciences*, 63 (2020) 65.
5. K. Qu, L. Wei and Q. Zou, *Current Bioinformatics*, 14 (2019) 246.
6. X. Du, C. Zhao, S. Liu and S. Su, *Pakistan journal of medical sciences*, 36 (2020) 501.
7. V. Popa, D. Teculescu, D. Stanescu and N. Gavrilescu, *Diseases of the Chest*, 56 (1969) 395.
8. J. Hu, H. Zhang, L. Liu, X. Zhu, C. Zhao and Q. Pan, *IEEE Transactions on Robotics*, 36 (2020) 1805.
9. X. Xu and M. Nieto-Vesperinas, *Physical review letters*, 123 (2019) 233902.
10. D. Pan, X.-X. Xia, H. Zhou, S.-Q. Jin, Y.-Y. Lu, H. Liu, M.-L. Gao and Z.-B. Jin, *Stem cell research & therapy*, 11 (2020) 1.
11. X. Xu, Y. Yang, L. Chen, X. Chen, T. Wu, Y. Li, X. Liu, Y. Zhang and B. Li, *Laser & Photonics Reviews*, 15 (2021) 2000546.
12. J. Hu, H. Zhang, Z. Li, C. Zhao, Z. Xu and Q. Pan, *Asian Journal of Control*, (2020) 1.
13. S. Yang, Z. Li, K. Yan, X. Zhang, Z. Xu, W. Liu, Z. Liu and H. Liu, *Journal of Environmental Sciences*, 103 (2021) 59.
14. V.D. Singh and S.J. Daharwal, *Research Journal of Pharmacy and Technology*, 7 (2014) 1208.
15. P. Pai, N. Lalitha, B. Balakrishna and G. Rao, *Indian journal of pharmaceutical sciences*, 68 (2006) 501.
16. B. Zhang, D. Ji, D. Fang, S. Liang, Y. Fan and X. Chen, *IEEE Electron Device Letters*, 40 (2019) 780.
17. H.P. Uskaikar, N.P. Shetti, S.D. Bukkitgar, S.J. Malode, N.V. Jamakandi and T. Manu, *Materials Today: Proceedings*, 18 (2019) 963.
18. K.C. Naik, N.P. Shetti, S.D. Bukkitgar, S.J. Malode and H.P. Uskaikar, *Materials Today: Proceedings*, 18 (2019) 941.
19. S.D. Bukkitgar, N.P. Shetti, R.S. Malladi, K.R. Reddy, S.S. Kalanur and T.M. Aminabhavi, *Journal of Molecular Liquids*, 300 (2020) 112368.
20. C. Wang, X. Zhu, L. Zhang, Q. Song, H. Xu and X. Liu, *International Journal of Electrochemical Science*, 16 (2021) 210435.
21. W. Wang and D. Sun, *International Journal of Electrochemical Science*, 16 (2021) 210216.
22. J. xi Ma, L. Yang, L. Wang, S.Q. Wu and Y. Liu, *International Journal of Electrochemical Science*, 16 (2021) 150922.
23. V. Srinivas, C.V. Moorthy, V. Dedeepya, P. Manikanta and V. Satish, *Heat and Mass Transfer*, 52 (2016) 701.
24. K. Ghanbari and M. Moloudi, *Analytical biochemistry*, 512 (2016) 91.
25. K.C. Jha, Z. Liu, H. Vijwani, M. Nadagouda, S.M. Mukhopadhyay and M. Tsige, *Molecules*, 21 (2016) 953.

26. S. Boscarino, S. Filice, A. Sciuto, S. Libertino, M. Scuderi, C. Galati and S. Scalese, *Nanomaterials (Basel, Switzerland)*, 9 (2019) 1099.
27. R.K. N.B., V. Crasta, B.M. Praveen and M. Kumar, *Nanotechnology Reviews*, 4 (2015) 457.
28. H. Savaloni and R. Savari, *Materials Chemistry and Physics*, 214 (2018) 402.
29. X. Wang, Z. Feng, B. Xiao, J. Zhao, H. Ma, Y. Tian, H. Pang and L. Tan, *Green Chemistry*, 22 (2020) 6157.
30. Y. Matsuda, J. Tahir-Kheli and W.A. Goddard III, *The Journal of Physical Chemistry Letters*, 1 (2010) 2946.
31. Y. Liu, J. Zhang, Y. Cheng and S.P. Jiang, *ACS omega*, 3 (2018) 667.
32. H. Savaloni, E. Khani, R. Savari, F. Chahshouri and F. Placido, *Applied Physics A*, 127 (2021) 1.
33. H. Savaloni, R. Savari and S. Abbasi, *Current Applied Physics*, 18 (2018) 869.
34. R. Savari, H. Savaloni, S. Abbasi and F. Placido, *Sensors and Actuators B: Chemical*, 266 (2018) 620.
35. A. Ayeshamariam, D. Saravanakkumar, M. Kashif, S. Sivaranjani and B. Ravikumar, *Mechanics of Advanced Materials and Modern Processes*, 2 (2016) 3.
36. F. Qiu, G. He, M. Hao and G. Zhang, *Materials (Basel, Switzerland)*, 11 (2018) 2139.
37. N. Shakeel, M.I. Ahamed, S. Kanchi and H.A. Kashmery, *Scientific reports*, 10 (2020) 1.
38. W. Bao, Z. Deng, S. Zhang, Z. Ji and H. Zhang, *Frontiers in Materials*, 6 (2019) 72.
39. A. Levent, Y. Yardım and Z. Şentürk, *Sensors and actuators B: Chemical*, 203 (2014) 517.
40. B.T. Demircigil, B. Uslu, Y. Özkan, S.A. Özkan and Z. Sentürk, *Electroanalysis: An International Journal Devoted to Fundamental and Practical Aspects of Electroanalysis*, 15 (2003) 230.
41. J.-J. Sun, Y. Wu and J.-F. Song, *Electrochimica Acta*, 115 (2014) 386.
42. Y. Piao, *International Journal of Electrochemical Science*, 7 (2012) 6084.